Theoretical analysis and optimization of 3D laser beam shaping

M. TRACZYK, J. WOJTANOWSKI*, Z. MIERCZYK, M. ZYGMUNT, P. KNYSAK,
T. DROZD, and M. MUZAL

Institute of Optoelectronics, Military University of Technology, 2 Sylwestra Kaliskiego St., 00-908 Warsaw, Poland

Abstract. We report methodology of three-dimensional laser beam shaping. The analytical and numerical analysis is presented. A strategy for designing optical system involves the controlled application of aberrations which is realized by specific aspheric lens shaping. The goal is to obtain the desired optical power density distribution in space, which is optimal for selected application. The proposed method is discussed with regard to the design of optical transmitter for laser shooting simulator, however the developed methodology can be used for a number of other light shaping applications.

Key words: laser beam shaping, optical aberrations, non-imaging optics.

1. Introduction

Laser shooting simulators or weapon laser simulators (WLS) are systems used for training soldiers in conditions similar to a real battlefield. Such systems can simulate fire impact of nearly every kind of weapon used in modern army. Transmitters mounted on weapons simulate all real parameters of fire, such as ballistics, effective range, rate, ammo. Moreover, the information about the time of shot and shooter identification number is transmitted to the target, as well as the type of weapon which was used. This information allows detector system mounted on a soldier's uniform or generally on a target to make a decision about the shot effect. Depending on a weapon type and aiming precision, target can be damaged or destroyed. Situation such as tank destruction by small arms are prevented. Apart from transmitters and detectors, each training element is equipped with GPS and communication module transmitting information about the temporal location, status of ammunition, damages, hits and other parameters to the respective training center and commanders.

One of the most vital and challenging issues of laser simulators is to obtain the appropriate light distribution in space which depends on the type of ammo/weapon it simulates. Transmitters emitting laser radiation should meet specific requirements concerning output optical power density distribution in space. The ideal cross-section range resolved distribution of the light beam is shown in Fig. 1. OZ axis corresponds to distance and OY axis is associated with perpendicular direction and thus cross section of the beam. Solid line indicates the border of what can be called an active beam diameter. Power density inside this area is higher than prescribed threshold level ρ_{thr} established for triggering the detectors. In ideal case beam diameter is growing rapidly with distance to reach desired value D at the range of $R_{\min}$ and disappears after reaching a distance $R_{\max}$ which corresponds to a weapon operational range. An effective beam diameter is typically large enough to hit at least one detector on a target

and small enough to prevent activating detectors on separate targets which may be located side by side in close proximity.
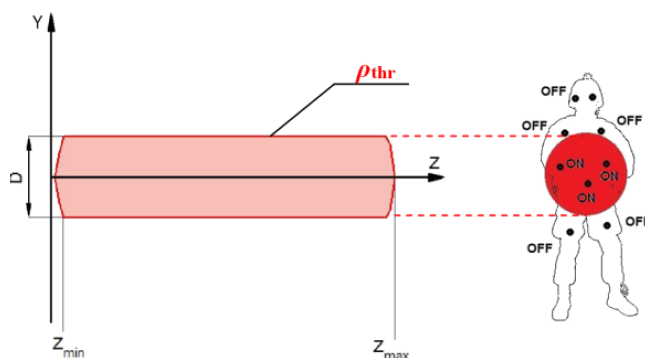

Fig. 1. General concept of beam forming for laser simulators – the desired effective cross section range distribution of laser beam and the arrangement of detectors (black dots) on a target

Previous solutions applied in WLS optical transmitters were frequently based on mechanically varying defocus of light source. Before shooting, this solution required evaluation of distance to the target, setting and positioning a mechanical lever accordingly. The proposed method does not require any shiftable mechanical components for beam formation. It is based purely on optical approach and the controlled injection of aberrations by the specific shape of optimized aspheric lens.

2. Optical modelling of transmitter

2.1. General setup of WLS transmitter and modelling approach. WLS transmitter consists of a laser source and a refractive collimating element – a lens (Fig. 2). The emitting structure of the laser is placed at the focal plane of the lens. The source is based in the object space coordinates system (x, y, z) and the target planes reside in the image space (X, Y, Z).

*e-mail: jwojtanowski@wat.edu.pl
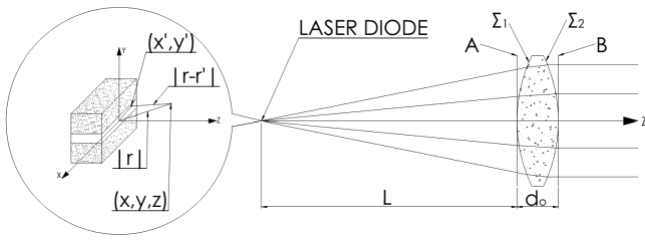
M. Traczyk et al.

Fig. 2. Setup of WLS transmitter

In the first stage of analysis, light distribution in "A" plane is calculated by modelling free space propagation from the laser source to the lens. Next step involves the calculation of light distribution in "B" plane, after passing through the collimating lens, which is obtained by introducing complex lens-shape-dependent phase shift added to the wavefront. The resulting distribution is then used to calculate the distribution of light at various target distances $Z_{\min}$, Z_1, Z_2 up to $Z_{\max}$. The last stage includes free space propagation modelling and incoherent convolution.

2.2. Theoretical model of WLS transmitter. The light source most often used in WLS transmitters is a semiconductor laser diode which provides astigmatic intensity profile with different angles of divergence and poor optical quality [1–3]. A general shape of the laser emitting structure is shown in Fig. 3. A single bar has dimensions of the order of tens of microns. The whole structure consists of several (M) bars. The half-angle beam divergence emitted from such a source are θ_p (XZ plane) and θ_r (YZ plane), $\theta_p < \theta_r$. Total power P_o emitted by the laser is a net effect of all contributing stripes.
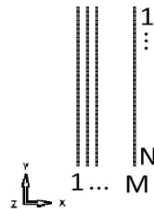

Fig. 3. General structure of semiconductor laser emitting stripes

Due to substantial size of bars and mechanism of emission, the output radiation is not fully spatially coherent, thus methods typically used to describe coherent sources and wavefronts need to be modified. In the proposed approach one assumes a single laser bar as a set of coherent sub-sources, each sized Δx x Δy μm an with half-divergence angles θ_p and θ_r. The total intensity of the laser diode can be expressed by:

$$I_C(x,y,z) = a \sum_{i=0}^{M} \sum_{j=0}^{N} [u_S(x - b_j, y - c_i)]^2, \qquad (1)$$

where u_s is a single sub-emitter contribution, a is normalizing constant, (b_j, c_i) determine the position of a single source in the object (focal) plane. Considering any specific laser chip and its dimensions, one can divide emitting stripes into varying number of sub-sources and thus define their size.

To obtain the light distribution on the front side of the collimating lens, free-space propagation from each individual laser sub-source to the plane A was modeled by the application of scalar diffraction theory. Light distribution observed at a distance much larger than the wavelength and the size of the source, which translates to $z \gg 0.5 \cdot k(\Delta^2 + \Delta^2)$ [4], optical field u resulting from single sub-source contribution can be described as the following diffraction integral:

$$u(x,y,z) = \frac{-iz}{\lambda r} \frac{\exp(ikr)}{r} \int \int u_S(x',y')$$
$$\exp\left[\frac{-ik}{r}(xx' + yy')\right] dx'dy', \qquad (2)$$

where $r = (x^2 + y^2 + z^2)^{1/2}$. Semiconductor laser can be approached as a waveguide with highly asymmetric dimensional ratio [2, 5]. Distribution of the fundamental mode of the light field in face plane of laser chip can be then expressed by:

$$u_S(x', y')$$
$$= u_0 \left[1 + \sum_m c_{2m} H_{2m}(\sqrt{2}qy') \exp(-p\,|x'|) - q^2 y'^2\right], \qquad (3)$$

where p and q are constants related to the structure of the laser waveguide, H_{2m} is a Hermite polynomial of order $2m$, c_{2m} is a constant factor. Substituting Eq. (3) to Eq. (2) one can obtain the distribution of light generated by the semiconductor diode in the far field [5–7]:

$$u(x,y,z) = A \frac{z}{r} \frac{\exp(ikr)}{r} F\left(\frac{\sqrt{2}y}{\Omega}\right) \frac{\Gamma^2}{\Gamma^2 + x^2}$$
$$\exp\left(\frac{-2y^2}{\Omega^2}\right), \qquad (4)$$

where

$$F\left(\frac{\sqrt{2}y}{\Omega}\right) = 1 + \sum_m (-1)^m c_{2m} H_{2m}\left(\frac{\sqrt{2}y}{\Omega}\right), \qquad (5)$$

$$A = -u_0 \frac{2i}{\lambda p} \left(\frac{\pi}{q}\right)^{1/2}, \qquad (6)$$

$$\Gamma^2 = \left(\frac{p^2}{k^2}\right) r^2, \qquad (7)$$

$$\Omega^2 = \left(\frac{4q^2}{k^2}\right) r^2. \qquad (8)$$

To verify this approach, numerical modeling was challenged by comparison with experimental results. Light distribution obtained from the selected laser diode in the far field and computational results are presented side by side in Fig. 4.
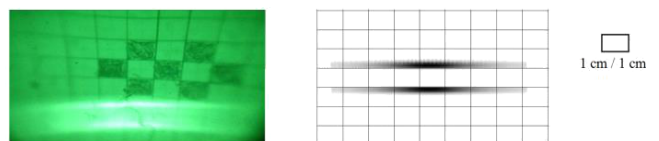

Fig. 4. Experimental (left) and numerical simulation result (right) regarding light intensity distribution at the distance of 0.1 m obtained from the selected laser diode

Values of parameters $q = 1.5 \cdot 10^6$ m^{-1} and $p = 0.3 \cdot 10^6$ m^{-1} corresponding to emitting structure geometry of the laser applied were used in calculation. Knowing the light distribution directly in front of a lens (plane A), one can easily obtain its pattern just behind it (in plane B) [8]:

$$u_B = u_A(x,y,z)\exp(i\Phi(x,y)), \qquad (9)$$

where $\Phi(x,y)$ is the phase delay introduced to a wavefront by a lens in point (x,y). This phase factor corresponds to the local thickness of the lens which can be expressed by [8, 9]:

$$\Phi(x,y) = kd_0 + k(n-1)d(x,y), \qquad (10)$$

where d_0 is the thickness of the lens along the optical axis $(x=0, y=0)$, $d(x,y)$ is the lens thickness at (x,y) point, n is the relative refractive index of the lens glass. Thickness $d(x,y)$ of an even single-sided aspheric lens is expressed by the following formula:

$$\begin{aligned} d(x,y) = d_0 &- \frac{c_1(x^2+y^2)}{1+\sqrt{1-c_1^2(x^2+y^2)^2}} \\ &+ \frac{c_2(x^2+y^2)}{1+\sqrt{1-(1-k_2)c_2^2(x^2+y^2)^2}} + ... \\ &... + A_2(x^2+y^2)^2 + A_4(x^2+y^2)^4 \\ &+ A_6(x^2+y^2)^6 + ... \end{aligned} \qquad (11)$$

where $c_{1,2} = R_{1,2}^{-1}$ is a curvature of the first and second surface respectively, k is the conic constant, $(A_2, A_4, A_6,...)$ are aspheric coefficients. The above mentioned parameters determine the shape of the lens and thus are associated with wavefront aberrations [1, 4] affecting light power density distribution in the far field. Optical amplitude in the plane "B" resulting from a single coherent sub-source can then be obtained by:

$$\begin{aligned} u_B(x,y) = &A\frac{L}{r}\frac{\exp(ikr)}{r}F\left(\frac{\sqrt{2}y}{\Omega}\right)\frac{\Gamma^2}{\Gamma^2+x^2} \\ &\exp\left(\frac{-2y^2}{\Omega^2}\right)\exp(ikd_0+ik(n-1)d(x,y)), \end{aligned} \qquad (12)$$

where L is the distance from laser diode to the lens front surface.

2.3. Modeling the light intensity distribution in target planes – convolution method. To obtain the optical power density distribution in the image space, one has to propagate the wavefronts from the output of transmitter to the target planes located at selected distances Z_i. The optical power is the object of interest since it corresponds directly to the current in square-law photonic detectors [10]. The applied method is based on distribution of the initial light field into the plane waves with different amplitudes and angles of propagation (angular spectrum of plane waves). These waves propagate independently to the target range [11]. The final light distribution is the result of the superposition of all waves.

The optical field $u_Z(X,Y,Z)$ at a distance Z, resulting from initial distribution which in the case discussed is $u_B(x,y)$ may be assumed as a convolution of the latter with the impulse response of free space h:

$$u_Z(X,Y,Z) = u_B(x,y,z) \otimes h(X,Y,Z,\lambda), \qquad (13)$$

where h is defined by [12]:

$$h(X,Y,Z,\lambda) = \frac{\exp(ikZ)}{i\lambda Z}\exp\left[\frac{ik}{2Z}(X^2+Y^2)\right]. \qquad (14)$$

Mathematically, it is reasonable to perform a convolution in Fourier domain where it transforms to ordinary multiplication. A return to the original space is then achieved by inverse Fourier transform. This approach was adopted in the computations of light distribution in (X, Y, Z) space (Fig. 5).
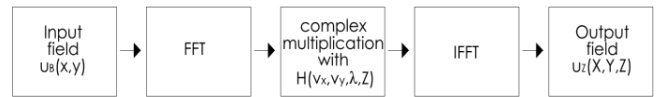

Fig. 5. A block diagram illustrating the steps of convolution metho

In the above scheme, H is the Fourier transform of the free space impulse response function h, namely:

$$\begin{aligned} H(v_x, x_y, \lambda, Z) &= F\left[h(x,y,\lambda,Z)\right] \\ &= \exp(ikZ)\exp\left[\frac{-iZ}{2k}(v_x^2+v_y^2)\right], \end{aligned} \qquad (15)$$

where v_x and v_y are spatial frequencies. Light intensity distribution at the distance Z resulting from single (i, j) sub-source can be obtained by conjugated multiplication of the corresponding optical field:

$$I_{i,j}(X,Y,Z) = U_{Zi,j}(X,Y,Z)U_{Zi,j}^*(X,Y,Z). \qquad (16)$$

The total output intensity I_C which takes into account the contribution of all coherent sub-sources is calculated as an incoherent sum of their intensities $I_{i,j}$:

$$I_C(X,Y,Z) = \sum_{i=0}^{M}\sum_{j=0}^{N}I_{i,j}(X,Y). \qquad (17)$$

As mentioned, the effective beam diameter D at any distance Z is determined not by classical e^{-2} criterion, but corresponds to the absolute power density threshold ρ_{thr} (Fig. 6).
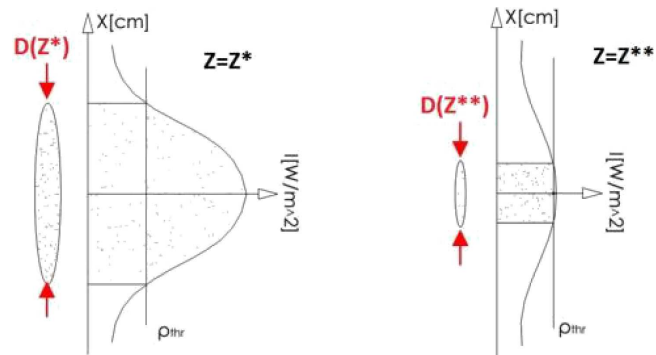

Fig. 6. Size (diameter) of the beam – intensity threshold methodology (note: at both distances $(Z*, Z**)$ beam shows the same e^{-2}-*criterion* diameter which is in opposition to ρ_{thr}-*criterion* approach)

In order to obtain the range distribution of the effective diameter $D(Z)$, light power density pattern at the selected distances Z_1, Z_2, ... Z_{max} was calculated. It enabled to determine the impact of lens asphericity on optical power density threshold isolines. In case of rotationally symmetric problem, 2-D isoline $I(X,Z) = \rho_{thr}$ is also the representation of 3-D isosurface $I(X,Y,Z) = \rho_{thr}$. On the other side, if asymmetry exists, one should consider at least two planes separately.

3. Optimization

Matlab [13] environment was used to perform the numerical analysis of the problem discussed. Obtained formulas have been implemented and computationally optimized. Additionally, a merit function used for optimization was created. During the optimization, light was propagated to the set of equally spaced distances from Z_{min} to Z_{max} with increments of ΔZ, where intensity profiles were analyzed to obtain the respective beam diameters. Algorithm modified the following variables: diameter of the lens D_0, distance between the lens and the source L, laser power P_0 and lens asphericity coefficients: k, A_2, A_4, A_6, A_8. The sum of errors ΔZ_n, corresponding to the absolute difference between the calculated and desired D value for every distance Z_n, was considered as a merit number.
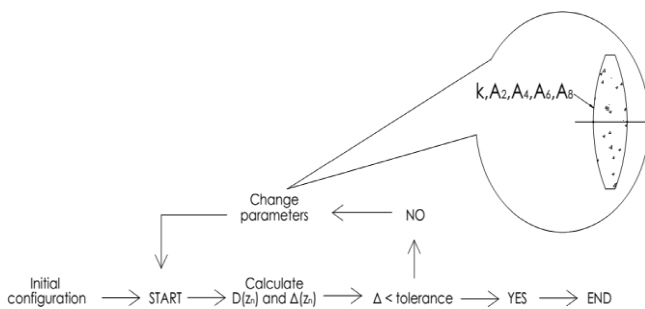

Fig. 7. Diagram of the optimization process

The optimization module changed the parameters and the process of calculation was repeated until the total error level dropped below a given threshold or further changes in the coefficients values did not significantly influence the performance.

4. Case study – laser transmitter for "Beryl 96" rifle WLS

WLS laser transmitter dedicated to the assault rifle with an effective range of 400 m is discussed as an example. The design goal is to form a light beam with an effective diameter of 45 cm at the distance from 1 m to 400 m. The desired diameter results from the deployment of the detectors on potential targets and their dimensions. As discussed, the beam diameter cannot be too small, as the laser beam might hit the area

between the adjacent detectors without causing any effect. Its size cannot be too high due to the probability of neutralizing multiple targets with a single shot. Both cases are unrealistic and should be prevented. Concerning the power density threshold level, it was assumed to be 1.5 Wm^{-2} which corresponds to current state-of-the-art systems. Transmitter consists of a commercially available pulsed 905 nm laser diode. Laser emitting chip structure corresponds to Fig. 3, where $N = 75$ is considered. Accordingly, 15×75 μm chip consists of three stripes, each of 1×75 μm size. The half-angle divergences of the original laser beam are 10° vs. 25° in ZX and ZY planes respectively. At the initial configuration, 10 W laser diode is placed at the focus of collimating BK7 commercial spherical lens with a focal length $f = 75$ mm, diameter $D_0 = 12.7$ mm and central thickness $d_o = 4.12$ mm. The distribution of threshold intensity isolines created by the initial configuration of the transmitter is presented in Fig. 8. It's evident, that this configuration does not satisfy the requirements that were specified.
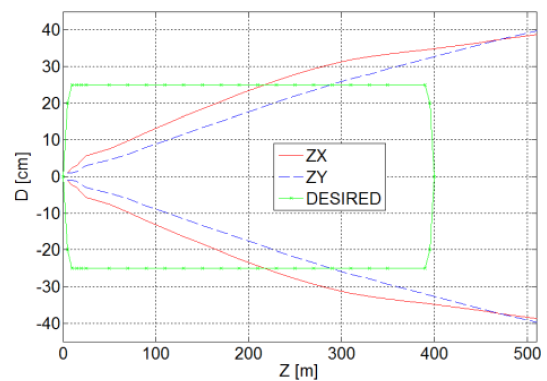

Fig. 8. Range distribution of power density threshold isolines created by a spherical lens (orthogonal ZX and ZY planes were considered)

Different symmetrical and asymmetrical spherical lenses were tested, without any good results. Transmitter performance still remains unacceptable when a slight defocus is introduced (Fig. 9) to initial configuration, which would probably be the easiest (and cheapest) way to optimize the system.
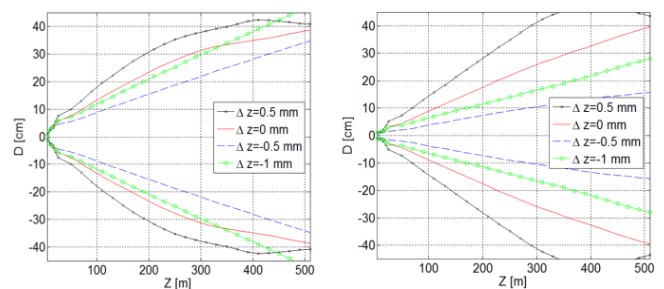

Fig. 9. Effective beam cross sections in ZX plane (left) and in ZY plane (right) in case of various defocus levels Δz introduced into initial configuration

Theoretical analysis and optimization of 3D laser beam shaping

Table 1
Optimized asphericity coefficients values for the lens and optical system setup

k [1]	A_2 [m^{-3}]	A_4 [m^{-7}]	A_6 [m^{-11}]	A_8 [m^{-15}]	L [mm]	D_o [mm]	P_o [W]
5	$-9.85 \cdot 10^{-5}$	$7.47 \cdot 10^{-6}$	$-7.97 \cdot 10^{-7}$	$-8.54 \cdot 10^{-10}$	72	12.7	14

Therefore, aspheric technology appeared to be a promising candidate. The developed method becomes a functional tool to find the aspheric shape providing the desired 3-D distribution of light intensity. During the optimization process, after each loop the algorithm changed the set of optical parameters, minimizing the total error Δ, which resulted in approaching the desired beam shape. The exact numerical values of the calculated coefficients for optimized lens are presented in Table 1.

It should be noted that the obtained numbers indicate highly aberrated optical performance. The total *rms* wavefront error at the level of 7.3 λ absolutely discriminates the calculated aspheric lens in the area of classical imaging applications [9, 14]. Spatial distribution of the effective beam diameter provided by the optimized element (Fig. 10) seems to be satisfactory in the application discussed. Comparing to initial "spherical" performance, a significant improvement has been attained.
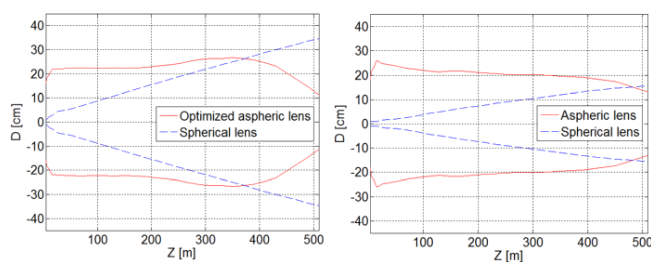

Fig. 10. Range distribution of the calculated effective beam diameter in *ZX* plane (left) and *ZY* plane (right) for the optimized lens (solid line) and initial standard spherical lens (dashed line)

Potentially, it is possible to approach the "perfect case" even closer, however it requires time-consuming calculations and/or more computing power. The asymmetrical features of the beam in both orthogonal planes result from the substantial discrepancy in laser emitting structure dimensions in $0x$ and $0y$ directions. The application of more symmetrical input beam profile (i.e. fiber coupled laser) would heal this effect.

5. Verification of the results

To validate the obtained results, Zemax software [15] was implemented. It is a worldwide recognized environment used by institutions and companies in the optical industry to assist the analysis of optical systems. The appropriate comparison is presented in Fig. 11. Intensity cross-section calculated by Zemax and resulting threshold-related diameters are in full agreement with the beam profile obtained via the proposed method. This agreement was proved to be valid both for initial spherical and optimized aspheric optics.
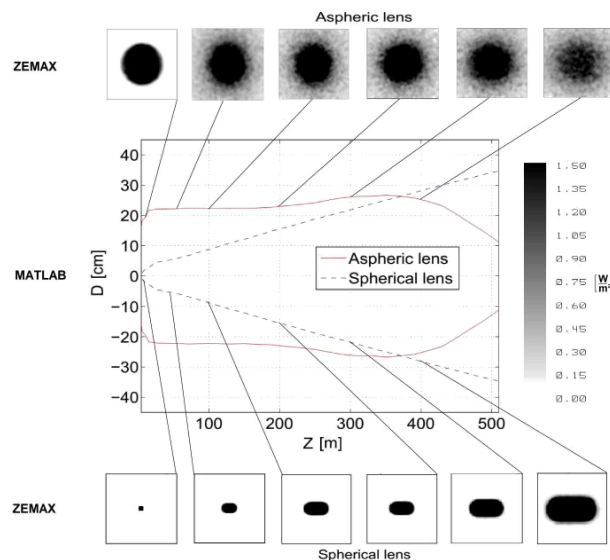

Fig. 11. Verification of the results. Apart from the calculated beam profiles (also in Fig. 10), intensity cross-sections obtained in Zemax are presented both for spherical (initial) lens and optimized aspheric one

6. Conclusions

The modelling and optimization method for laser beam shaping was presented It proved to meet the specific optical design intent associated with problematic WLS transmitters – to calculate aspheric refractive component which will provide cylinder-alike distribution of the given optical power density threshold in space. Traditional spherical and aspheric components do not meet such requirements and their application in the discussed system is a far-reaching compromise. It needs to be mentioned, that the optical performance of WLS transmitters appeared to be totally different from conventional imaging systems where aberrations are minimized. Therefore, elements of this type are not commercially available and need to be designed/ordered on request. Nevertheless, the fabrication technology of exotic aspheric components is becoming more and more available and cheap. Simulators of weapons are definitely among those types of equipment which should take advantage of the high-end technology and solutions. The proposed method can be successfully applied in other fields as well (car headlights design, illumination systems, free-space communication, *Friend or Foe* identification systems, lidar systems and others).

REFERENCES

[1] M. Born, E. Wolf, *Principles of Optics*, Cambridge University Press, Cambridge, 2003.
[2] H. Sun, *Laser Diode Beam Basics, Manipulations, and Characterizations*, Springer, New York, 2012.

[3] A. Maląg, "Beam divergence and COD issues in double barrier separate confinement heterostructure laser diodes", *Bull. Pol. Ac.: Tech.* 53 (2), 167–173 (2005).

[4] R. Jóźwicki, *Instrumental Optics*, Scientific-Technical Publisher, Warsaw, 1970, (in Polish),

[5] T.H. Zachos and J.E. Ripper, "Resonant modes of GaAs junction lasers", *IEEE J. Quantum Electron.* QE-5, 29–37 (1969).

[6] X. Zeng and A. Naqwi, "Far-field distribution of double-heterostructure diode laser beams", *Appl. Opt.* 32 (24), 4491–4494 (1993).

[7] S. Nemoto, "Experimental evaluation of a new expression for the far field of a diode laser beam", *Appl. Opt.* 33 (27), 6387–6392 (1994).

[8] X. Qiang, H. Yiping, and C. Zhiwei, "Characteristic of laser diode beam propagation through a collimating lens", *Appl. Opt.* 49 (3), 549-553 (2010).

[9] J.K. Jabczyński, *Fundamentals of Instrumental Optics*, Military University of Technology, Warsaw, 2006, (in Polish).

[10] A. Rogalski and Z. Bielecki, "Detection of optical radiation", *Bull. Pol. Ac.: Tech.* 52 (1), 43–66 (2004).

[11] J. Petykiewicz, *Wave Optics*, Publishing House of Warsaw University of Technology, Warsaw, 1978, (in Polish).

[12] M. Sypek, "Light propagation in the Fresnel region. New numerical approach", *Optics Comm.* 116, 43–48 (1995).

[13] http://www.mathworks.com/products/matlab/

[14] M. Zając, *Aberration of Hybrid Optical Imaging Systems*, Publishing House of Wroclaw University of Technology, Wroclaw, 2005, (in Polish).

[15] http://www.radiantzemax.com